Unclassified

COPY

(2)

DOCUMENTATION PAGE

Form Approved OMB No. 0704-0188

AD-A222 086 DTIC ELECTE MAY 29 1990 S D Cs

1b. RESTRICTIVE MARKINGS	
2a. SECURITY CLASSIFICATION AUTHORITY	3. DISTRIBUTION/AVAILABILITY OF REPORT: Approved for public release; distribution is unlimited.
2b. DECLASSIFICATION/DOWNGRADING SCHEDULE	
4. PERFORMING ORGANIZATION REPORT NUMBER(S)	5. MONITORING ORGANIZATION REPORT NUMBER(S): AFOSR-TR- 90 0637
6a. NAME OF PERFORMING ORGANIZATION: National Institute of Standards and Technology	6b. OFFICE SYMBOL (If applicable):
6c. ADDRESS (City, State, and ZIP Code): Gaithersburg, MD 20899	7a. NAME OF MONITORING ORGANIZATION: AFOSR/NA
8a. NAME OF FUNDING/SPONSORING ORGANIZATION: AFOSR/NA	8b. OFFICE SYMBOL (If applicable): NA
8c. ADDRESS (City, State, and ZIP Code): Building 410, Bolling AFB DC 20332-6448	7b. ADDRESS (City, State, and ZIP Code): Building 410, Bolling AFB DC 20332-6448
	9. PROCUREMENT INSTRUMENT IDENTIFICATION NUMBER: AFOSR-ISSA-89-0025
	10 SOURCE OF FUNDING NUMBERS: PROGRAM ELEMENT NO. 61102F; PROJECT NO. 2308; TASK NO A2; WORK UNIT ACCESSION NO.

11. TITLE (Include Security Classification)
(U) Diffusion-Controlled Reaction in a Vortex Field

12. PERSONAL AUTHOR(S)
Ronald G. Rehm, Howard R. Baum, Daniel W Lozier, and Jonathan Aronson

13a. TYPE OF REPORT	13b. TIME COVERED	14. DATE OF REPORT (Year, Month, Day)	15. PAGE COUNT
Reprint	FROM _____ TO _____	December, 1989	26

16. SUPPLEMENTARY NOTATION

17 COSATI CODES			18. SUBJECT TERMS (Continue on reverse if necessary and identify by block number)
FIELD	GROUP	SUB-GROUP	Combustion modeling; flame sheet; reacting flow; Reprints. (jld)

19. ABSTRACT (Continue on reverse if necessary and identify by block number)

A two-dimensional model of a constant-density diffusion-controlled reaction between unmixed species initially occupying adjacent half-spaces is formulated and analyzed. An axisymmetric viscous vortex field satisfying the Navier-Stokes equations winds up the interface between the species as they diffuse together and react. A flame-sheet approximation of the rapid reaction is made using a mixture fraction dependent variable. The problem was originally proposed by F. Marble, who performed a local analysis and determined the total consumption rate along the flame sheet. The present paper describes a global similarity solution to the problem which is Fourier analyzed in a Lagrangian coordinate system. The Fourier amplitudes are determined both by an asymptotic analysis, valid for large Schmidt numbers, and by numerical solution of the two-point boundary-value ordinary differential equations. The solution is evaluated in both Lagrangian and Eulerian coordinate systems. Comparisons are made between the asymptotic and the numerical solutions for a variety of values of the governing parameters, the Reynolds and Schmidt numbers. (Keywords:)

20. DISTRIBUTION/AVAILABILITY OF ABSTRACT	21. ABSTRACT SECURITY CLASSIFICATION
☒ UNCLASSIFIED/UNLIMITED ☒ SAME AS RPT ☐ DTIC USERS	Unclassified
22a. NAME OF RESPONSIBLE INDIVIDUAL: Julian M Tishkoff	22b TELEPHONE (Include Area Code): (202) 767-4965 (4467) / 22c. OFFICE SYMBOL: AFOSR/NA

DD Form 1473, JUN 86 Previous editions are obsolete. SECURITY CLASSIFICATION OF THIS PAGE

Unclassified

Combust Sci and Tech, 1989, Vol 66, pp. 293-317
Reprints available directly from the publisher
Photocopying permitted by license only

(Gordon and Breach Science Publishers, Inc.
Printed in Great Britain

Diffusion-Controlled Reaction in a Vortex Field

RONALD G. REHM, HOWARD R. BAUM,
DANIEL W. LOZIER and JONATHAN ARONSON *National Institute of Standards and Technology (formerly the National Bureau of Standards) Gaithersburg, MD 20899, USA*

(Received January 11, 1989; in final form August 14, 1989)

Abstract—A two-dimensional model of a constant-density diffusion-controlled reaction between unmixed species initially occupying adjacent half-spaces is formulated and analyzed. An axisymmetric viscous vortex field satisfying the Navier-Stokes equations winds up the interface between the species as they diffuse together and react. A flame-sheet approximation of the rapid reaction is made using a mixture fraction dependent variable. The problem was originally proposed by F. Marble, who performed a local analysis and determined the total consumption rate along the flame sheet. The present paper describes a global similarity solution to the problem which is Fourier analyzed in a Lagrangian coordinate system. The Fourier amplitudes are determined both by an asymptotic analysis, valid for large Schmidt numbers, and by numerical solution of the two-point boundary-value ordinary differential equations. The solution is evaluated in both Lagrangian and Eulerian coordinate systems. Comparisons are made between the asymptotic and the numerical solutions for a variety of values of the governing parameters, the Reynolds and Schmidt numbers.

1 INTRODUCTION

The theoretical study of chemical reactions in complex flow fields, for example turbulent reacting flows, has received increased attention lately, for example Libby and Williams (1980), Williams (1985), Buckmaster and Ludford (1982, 1983), Oran and Boris (1981), Oppenheim (1986) and Ashurst (1987). This attention is warranted not only because numerical and analytical progress is being made in addressing the problem, but also because a much clearer physical picture of turbulent flows and their coupling to combustion processes has been achieved through experiments over the past fifteen years, Brown and Roshko (1974), Roshko (1976), Mungal and Dimotakis (1984) and Browand (1986). Turbulent combustion is difficult to analyze because it is highly nonlinear, transient and involves a wide range of length and time scales. When the Reynolds number is large, experiments indicate that the length and time scales associated with turbulent combustion can be separated by phenomenon into large and small scales. The large, or geometrical, scale is essentially inviscid or nondissipative and is related to the geometry defining the flow configuration and the fuel and oxidizer distributions. Combustion, on the other hand, takes place on the small scale associated with the diffusion of fuel and oxidizer into each other ", 'rides on" the geometrical scale and establishes the rate at which the reactants disappear and heat is released.

An outline of an approach for studying the problem of turbulent reacting flows, based on these observations and using both analytical and numerical methods, is given in a paper by Baum, Corley and Rehm (1986). The approach is to analyze large-scale flow fields separately from the small-scale mixing and reaction using the observation that these processes occur on widely differing length and time scales for large Reynolds numbers. The component problems are treated individually, but in a way that will allow the phenomena to be coupled through analytical and computational techniques. A model for three-dimensional small-scale mixing and reaction in a stretched vortex flow field is also presented; this model includes

the critical features for turbulent combustion of flame stretching and the three-dimensional effect of vortex stretching.

Marble (1985) originally posed a similar but more specialized two-dimensional model problem of small-scale mixing and reaction and studied it analytically. His model includes the two-dimensional effect of flame stretching, and was analyzed using methods presented earlier by Carrier, Fendell and Marble (1975) locally along the flame front to provide global dependences of the fuel and oxidizer consumption rates upon the governing parameters. The Marble problem has several important features: it is a diffusion-controlled reaction in a viscously spreading vorticity field which stretches the flame sheet. Even though it is only two dimensional, it approximates chemical reactions in individual vortices which occur in shear-layer mixing experiments, such as those of Mungal and Dimotakis (1984). Generalizations of the Marble problem for a stretched vortex flow field and for reactions which release heat, using a local analysis, have been performed by Karagozian (1982) and Karagozian and Marble (1986). Norton (1983) has extended these analyses to include effects of finite-rate chemistry.

Two-dimensional numerical computations of the flow properties in reacting mixing layers have recently been carried out by Riley, Metcalf and Orszag (1986), McMurtry *et al.* (1986), McMurtry (1987), McMurtry and Riley (1987) and Ghoniem and Givi (1987). In these computations and the experiments they simulate, two fluids, one containing fuel and the other containing oxidizer and each flowing unidirectionally with its own velocity are brought into contact at a "splitter plate". Downstream of the point of contact, the two fluids mix and chemical reactions take place as they diffuse together. Experiments indicate that during the early stages of development of these mixing layers, the flow fields remain primarily two dimensional. Then, before vortex pairing begins, the Marble problem can be regarded as an analytical approximation to combustion in one of the vortices. Also, recently, a direct numerical computation of the Marble problem has been presented by Laverdant and Candel (1988a, b), confirming the dependence of the global generation of products upon Reynolds number obtained originally by Marble (1985).

The work presented in this paper is essentially analytical, and, within the context of the mathematical model, permits one to calculate combustion properties much more accurately for given computational resources than direct numerical solution. Therefore, it could be used, for example, to test the accuracy of the numerical computations cited above, and it will be used to test methods for solutions to the more general problems described in Baum, Corley and Rehm (1986). The novel features of our work are (i) it is observed that the convection-diffusion equation for the mixture fraction variable permits a similarity solution, reducing the number of independent variables from three (radius, angle and time) to two (angle and similarity variable); (ii) as in Baum, Corley and Rehm (1986), a Langrangian coordinate system is used to eliminate flame-sheet resolution problems induced by vortex winding; (iii) Fourier analysis in angle and a combined numerical and analytical treatment in the similarity variable allow one to solve the global problem essentially exactly. Attention is given to graphical presentation of results of these analyses as functions of the two governing parameters, the Reynolds and the Schmidt numbers. Also, comparisons are made between the numerical solutions obtained here and the large-Schmidt-number asymptotic analysis presented.

In Section 2 we formulate the problem and give its complete mathematical description. In Section 3 an asymptotic solution, valid for large Schmidt numbers, is presented and a numerical solution of the problem is described. Also, a comparison between the two solutions is given in this section. In Section 4 we calculate the global fuel and

oxidizer consumption rates using the large Schmidt number analytical result and assuming in addition that the Reynolds number is large. Finally, in Section 5, some conclusions are drawn from this study.

2 FORMULATION OF THE PROBLEM

Consider the situation in which initially there is fuel in the left half-plane and oxidizer in the right half-plane in arbitrary proportions. These half-spaces are brought into contact and simultaneously a line vortex with axis at the origin is imposed (see Figure 1). The vortex induces a convective mixing of the interface between the two species, increasing the area of the separating surface in the neighborhood of the origin and enhancing the diffusion of the species into each other. It is assumed that the reaction rate is sufficiently rapid for the process to be limited by diffusion, and a flame-sheet approximation is made for the reaction. The chemical reaction is assumed to take place at constant density and all diffusion coefficients (kinematic viscosity, thermal and concentration coefficients) are assumed to be constant.

The governing equations for this problem are the Navier–Stokes equations and the species conservation equations. With the assumption that the density remains constant, these two sets of equations become decoupled, and a solution to the fluid equations can be determined and imposed on the species equations. A solution to the former equations is given by the tangential velocity for a diffusing line vortex of circulation Γ

$$v_\theta(r, t) = r\frac{d\theta}{dt} = \frac{\Gamma}{2\pi r}[1 - \exp(-\eta)] \tag{1}$$

where ν is the kinematic viscosity and $\eta = r^2/4\nu t$ is a similarity variable for the diffusing vortex.

The species conservation equations for the concentrations Y_1 and Y_2 are

$$\frac{\partial Y_i}{\partial t} + \frac{v_\theta}{r}\frac{\partial Y_i}{\partial \theta} = D\left(\frac{\partial^2 Y_i}{\partial r^2} + \frac{1}{r}\frac{\partial Y_i}{\partial r} + \frac{1}{r^2}\frac{\partial^2 Y_i}{\partial \theta^2}\right) - w \tag{2}$$

where $i = 1, 2$; D is the species diffusion coefficient which is assumed constant and the same for both species; v_θ is the imposed line-vortex azimuthal velocity; and w is

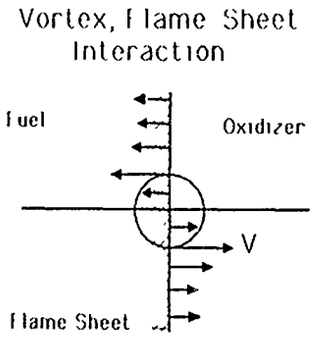

FIGURE 1 Schematic diagram of the Marble problem. Fuel, in the shaded left half-plane, and oxidizer in the right are allowed to react at the thin flame sheet separating them. Simultaneously, a line vortex with its axis at the origin induces convective mixing between the two species. The objective is to calculate the enhancement of the species consumption caused by the mixing.

the reaction rate, which is equal for both species. The initial conditions are that $Y_1 = Y_{10}$, $Y_2 = 0$ for $\pi/2 \leqslant \theta \leqslant 3\pi/2$ and $Y_1 = 0$, $Y_2 = Y_{20}$ for $-\pi/2 \leqslant \theta \leqslant \pi/2$, where we have taken Y_1 to be the concentration of fuel and Y_2 to be the concentration of oxidizer.

These equations represent a balance between convection, diffusion and reaction. If the reaction rate is sufficiently fast, it can be eliminated by taking a linear combination of the dependent variables with the assumption that the thermal and species diffusion coefficients are equal and the reactants cannot coexist. The linear combination of interest here is

$$Z = \frac{Y_1 - Y_2 + Y_{20}}{Y_{10} + Y_{20}} \tag{3}$$

The mixture-fraction variable Z satisfies the linear convection-diffusion equation

$$\frac{\partial Z}{\partial t} + \frac{v_\theta}{r}\frac{\partial Z}{\partial \theta} = D\left(\frac{\partial^2 Z}{\partial r^2} + \frac{1}{r}\frac{\partial Z}{\partial r} + \frac{1}{r^2}\frac{\partial^2 Z}{\partial \theta^2}\right) \tag{4}$$

The initial conditions are that $Z = 1$ for $\pi/2 \leqslant \theta \leqslant 3\pi/2$ and $Z = 0$ for $-\pi/2 \leqslant \theta \leqslant \pi/2$.

Integrating the tangential velocity gives the angle $\theta(r, \theta_0, t)$ at time t for any fluid element initially located at r, θ_0. A change of variables to the Lagrangian coordinates, ϱ, θ_0, τ,

$$\begin{aligned} r &= \varrho \\ \theta &= \theta_0 + \frac{\Gamma}{8\pi\nu}\frac{1 - E_2(\eta)}{\eta} \\ t &= \tau \\ E_i(z) &= \int_1^\infty t^{-i} \exp(-zt)\, dt \end{aligned} \tag{5}$$

can then be made in the equation for Z. Finally, assuming that Z is only a function of the similarity variable η and the angle θ_0, and performing a Fourier decomposition in the angle,

$$Z(\eta, \theta_0) = \sum_{n=-\infty}^{\infty} Z_n(\eta) \exp(in\theta_0) \tag{6}$$

a system of equations for each of the Fourier mode amplitudes Z_n is obtained:

$$\frac{d^2 Z_n}{d\eta^2} + f_n(\eta)\frac{dZ_n}{d\eta} + g_n(\eta) Z_n = 0 \tag{7}$$

where

$$f_n(\eta) = Sc + \frac{1}{\eta} + in\frac{1 - \exp(-\eta)}{\eta^2}\,\mathrm{Re}$$

$$g_n(\eta) = -\left(\left[\frac{1 - \exp(-\eta)}{\eta} Re\right]^2 + 1\right)\frac{n^2}{4\eta^2} + \frac{in}{2}\frac{\exp(-\eta) - [(1 - \exp(-\eta))/\eta]}{\eta^2} Re$$

and where $Sc = \nu/D$ is the Schmidt number and $Re = \Gamma/4\pi\nu$ is the Reynolds number based upon the circulation Γ.

The mathematical problem then reduces to the study of ordinary differential equations for Z_n in the similarity variable η. Boundary conditions are that the solution remain bounded as η goes to zero and that the initial conditions on Z_n are recovered as η goes to infinity. From the symmetry of the problem, the initial conditions are found to be, for even values of n, $Z_n(\zeta \to \infty) = 0$, and for odd values of $n = 2m + 1$,

$$Z_{2m+1}(\eta \to \infty) = \frac{(-1)^{m+1}}{\pi}\frac{1}{2m + 1} \tag{8}$$

The general solution for $Z_n(\eta)$ is a complex-valued function of the real variable η. From the governing equation, it is seen that $Z_{-n}(\eta)$ is the complex conjugate of $Z_n(\eta)$. The modes Z_n are synthesized using an FFT routine to determine $Z(\eta, \theta_0)$, and information about the location of the flame-sheet and the rate at which fuel is consumed can be determined.

A very special case can be used to test the numerical methodology and the computer programming. It also allows us to determine the boundary conditions in the similarity variable from initial conditions in the original variables. It is the pure diffusion case, which arises when the circulation Γ is taken to be zero. The known solution for the diffusion of two half-spaces into each other is given in terms of an error function,

$$Z_0(\eta, \theta_0) = (1/2)\,\mathrm{erfc}\,(\sqrt{Sc\eta}\cos\theta_0) \tag{9}$$

which is expressed in cylindrical coordinates and Fourier analyzed to give Z_n in terms of modified Bessel functions of integer order, $I_m(z)$.

$$Z_0(\eta, \theta_0) = A_0 + 2\sum_{m=0}^{\infty} A_{2m+1}(\eta)\cos[(2m + 1)\theta_0] \tag{10}$$

where $A_0 = 1/2$ and

$$A_{2m+1}(\eta) = \frac{(-1)^{m+1}}{\sqrt{2\pi}}\frac{1}{2m + 1}\sqrt{Sc\eta/2}\exp(-Sc\eta/2)\,[I_m(Sc\eta/2) + I_{m+1}(Sc\eta/2)] \tag{11}$$

This result has been used to examine the sensitivity of the numerical solution to the finite truncation of the infinite interval, to the number of terms retained in the Fourier synthesis of Z, and to the mesh size used in the solution of the two point boundary value problem, Eq. (7).

3 SOLUTIONS

3.1 *Large Schmidt Number*

When the Schmidt number is infinite, diffusion is unimportant and Eq. (4) is purely a convective equation in which the change of variables to Lagrangian coordinates reduces the problem to a trivial one. When the Schmidt number is large, asymptotic methods allow one to determine an approximate analytical solution to Eq. (7) from which the character of the solution to Eq. (4) for large Reynolds number can be determined. A change of dependent variable to $W_n(\eta)$ where

$$Z_n(\eta) = W_n(\eta) \exp\left(-Sc\eta/2 - \ln \eta/2 - (in\ Re/2)\,[E_2(\eta) - 1]/\eta\right) \tag{12}$$

gives the equation

$$\frac{d^2W_n}{d\eta^2} - F_n(\eta;\ Re,\ Sc)W_n(\eta) = 0 \tag{13}$$

where

$$F_n(\eta;\ Re,\ Sc) = \frac{(n^2 2 - 1)}{2\eta^2} + \frac{(Sc + 1/\eta)^2}{4} + \frac{in\ Re\ Sc}{2}\frac{(1 - e^{-\eta})}{\eta^2} \tag{14}$$

A singular perturbation analysis of Eq. (14) for large Sc yields two solutions $W_n^+(\eta)$ and $W_n^-(\eta)$, of which the former grows exponentially for large η, and the latter decays. The solutions, in turn, imply that the corresponding solutions $Z_n^+(\eta)$, $Z_n^-(\eta)$ become constant and decay exponentially for large η. Since the desired solution to Eq. (4) must pass to the pure-diffusion case for large η, we have

$$Z_{2m+1}^+(\eta \to \infty) \to \frac{(-1)^{m+1}}{\pi(2m + 1)} \tag{15}$$

and the constant multiple of $Z_{2m+1}^+(\eta)$ is determined. Since $Z_{2m+1}(\eta)$ decays exponentially as $\eta \to \infty$, any multiple of $Z_{2m+1}(\eta)$ can be added and we still have a solution. However, the solution for $Z_{2m+1}(\eta)$ must be bounded as $\eta \to 0$, and this fixes a linear combination of Z_{2m+1}^+ and Z_{2m+1}^-. Examination of Z_{2m+1}^+ to leading order in Sc shows that it is a constant throughout while the other solution is singular at $\eta = 0$ in the limit as $Sc \to \infty$. Hence Z_{2m+1}^+ is the desired solution.

Carrying out the asymptotic analysis for large Sc to next order yields

$$Z_{2m+1}^+(\eta) \cong \frac{(-1)^{m+1}}{\pi(2m + 1)} \exp\left[\frac{-(2m + 1)^2}{4Sc\eta}(A - iB)\right] \tag{16}$$

where

$$A = 1 + \frac{Re^2}{\eta^2}\left[\tfrac{1}{3} - 2E_4(\eta) + E_4(2\eta)\right]$$

$$B = \frac{2Re}{2m + 1}\left[\frac{-1}{2\eta} + \frac{E_3(\eta)}{\eta} + E_2(\eta)\right]$$

As $\eta \to \infty$, the argument of the exponential goes to zero and $Z^{+}_{2m+1}(\eta)$ goes to the appropriate constant, namely $(-1)^{m+1}/[2\pi(2m+1)]$. For small η, the asymptotic approximation $Z^{+}_{2m+1}(\eta)$ goes to zero as $\exp[-C/\eta]$ where C is a constant. We note that this asymptotic approximation is not uniformly valid in η as $\eta \to 0$. However, since the solution and the asymptotic approximation both approach zero, the difference between the two is small.

Substitution of Eq. (16) into Eq. (6) and performing some simplification yields the approximate solution to Eq. (4) for large Schmidt number:

$$\tilde{Z}(\eta, \theta_0) = 1/2 + 2 \sum_{m=0}^{\infty} \frac{\exp[-\tilde{A}_m(\eta)]}{\pi(2m+1)} \sin[(2m+1)\Phi_0] \tag{17}$$

where

$$\tilde{A}_m(\eta; Re, Sc) = (2m+1)^2 \frac{1 + Re^2 \tilde{f}_1(\eta)}{4Sc\,\eta}$$

$$\Phi_0 = \theta_0 \mp \frac{\pi}{2} - \frac{Re}{2Sc} \tilde{f}_2(\eta) \tag{18}$$

and where

$$\tilde{f}_1(\eta) = [1/3 - 2E_4(\eta) + E_4(2\eta)]/\eta^2$$

$$\tilde{f}_2(\eta) = [(E_3(\eta) - 1/2)/\eta + E_2(\eta)]/\eta$$

Here, the minus sign in Eq. (18) applies to the upper half plane and plus sign applies to the lower half plane.

Plots of functions $\tilde{f}_1$ and $\tilde{f}_2$ are shown in Figures 2a and 2b; they are smooth functions which allow us to determine the analytical behavior of $\tilde{Z}$ for large Schmidt numbers. For small η, $\tilde{f}_1 \to 1$ and $\tilde{f}_2 \to (1/2) \ln \eta$. For large η, $\tilde{f}_1 \to 1/(3\eta^2)$ and $\tilde{f}_2 \to -1/(2\eta)$.

Some important observations can be made from the asymptotic solution Eq. (17). First, note that $\tilde{Z} - 1/2$ is a Fourier sine series. When the sum of the terms in this series is small, the solution for the mixture-fraction variable is approximately 1/2. Since, for a stoichiometric mixture, $Z = 1/2$ is the equation for the flame sheet, the flame sheet for such a mixture occurs near where the sum of the Fourier series is small. Now, all terms of the series are exactly zero when $\Phi_0 = 0$, and this condition determines the equation for the flame sheet $\theta_0(\eta)$ for a stoichiometric mixture. However, the terms in the series will also be small when the argument of the exponential is large, and, when the Reynolds number is large, this occurs provided η is not too large.

The physical intepretation of these mathematical statements for large Reynolds and Schmidt numbers is as follows. For a stoichiometric mixture, there are two reaction regions. In the outer region there is a flame sheet, which remains close to the convectively mixed interface in the absence of diffusion. This interface is determined by the equation $\Phi_0 = 0$, and for moderately large η, is very close to $\theta_0 = \pm\pi/2$, which are the equations for the initial interface in the Lagrangian coordinate system. In the inner region, there is a burnt core in which both fuel and oxidizer are depleted, and the growth of this core is determined by the condition that the arguments of the

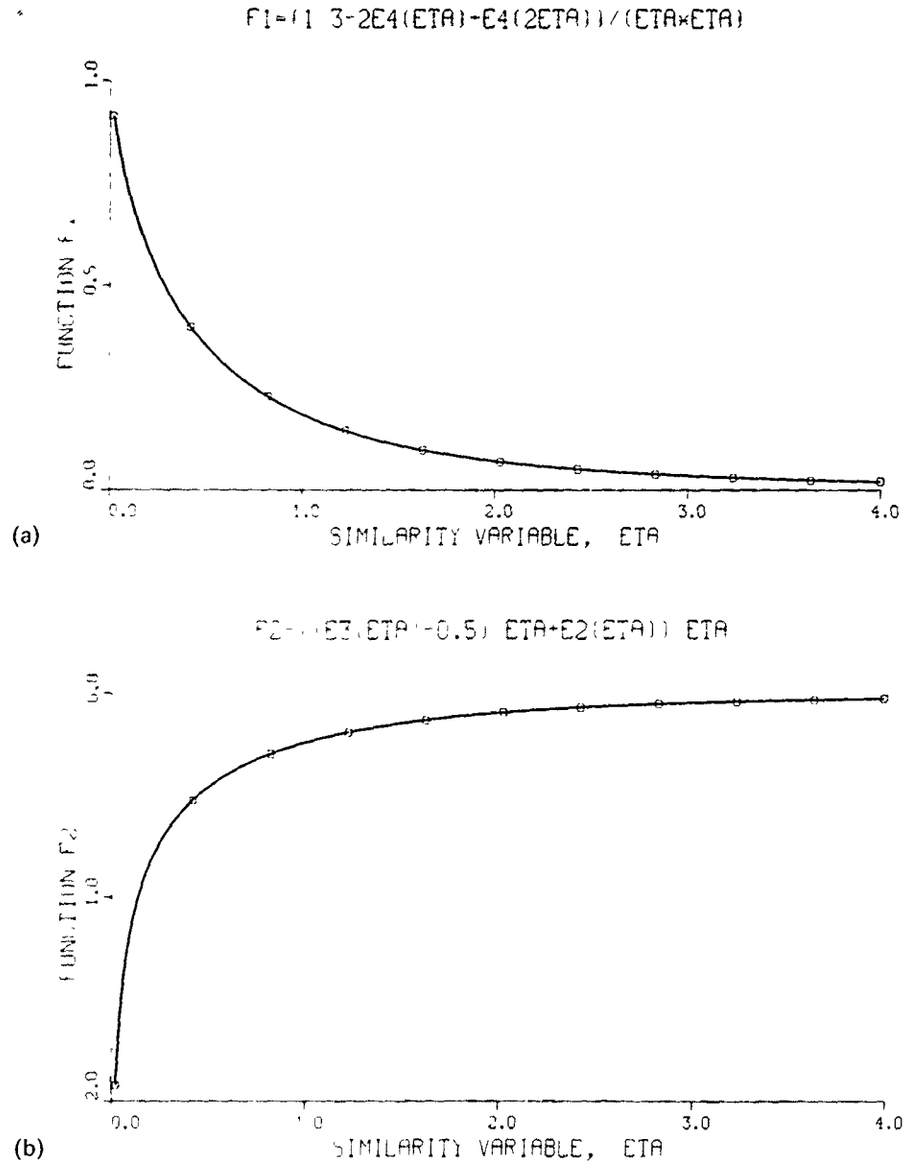

FIGURE 2 (a) Function $\tilde{f}_1(\eta)$ defined following Eq (18), the function arises in the large Schmidt number asymptotic analysis (b) Function $\tilde{f}_2(\eta)$ defined following Eq. (18), the function arises in the large Schmidt number asymptotic analysis

exponentials are large enough that each of the terms in the Fourier series is negligible. For a large Reynolds number (and Schmidt number) this condition determines a value of the similarity variable, η^* say, and the growth of the burnt core is determined then by the equation $r^2/4\nu t = \eta^*$. The observations about the burnt core are consistent with those made by Marble and Karagozian (1982, 1985, 1986).

A few words should be said about the large-Schmidt-number approximation. For gases, the Schmidt number is somewhat less than, but of the order of unity, whereas for liquids, it is typically much larger than one; see Appendix E of Williams (1985). Therefore, a large Schmidt number analysis should be applicable to liquids, but might be questionable for gases. However, it is often found that an asymptotic analysis has much wider applicability than would be indicated by the formal restrictions of the analysis. Therefore, one would expect that a large Schmidt number analysis will be qualitatively correct and perhaps even quantitatively correct also for gases. In Section 3.3, we make some comparisons between results obtained from the asymptotic analysis of this section and the numerical calculations of the next.

In Figure 3 is shown plots of the interface shape calculated from the large Schmidt number analysis for three values of the Reynolds number, 1, 10 and 100, in a Lagrangian coordinate system; these plots have been calculated for a Schmidt number of 10, which satisfies the requirement that the Schmidt number be large. These plots have the same scale, so that structures formed at larger Reynolds number extend to larger radius (or similarity variable η). For Reynolds number of unity, in Lagrangian coordinates, the interface hardly varies from a straight line. The circle around the origin shows the radius at which the burnt core is located (the location at which the amplitudes in Eq. (17) are down from the value 1/2 by exp (-3)). The two plots for larger Reynolds numbers, 10 and 100, show increased distortion of the interface around the origin and growth of the circle representing the burnt core. The distortion

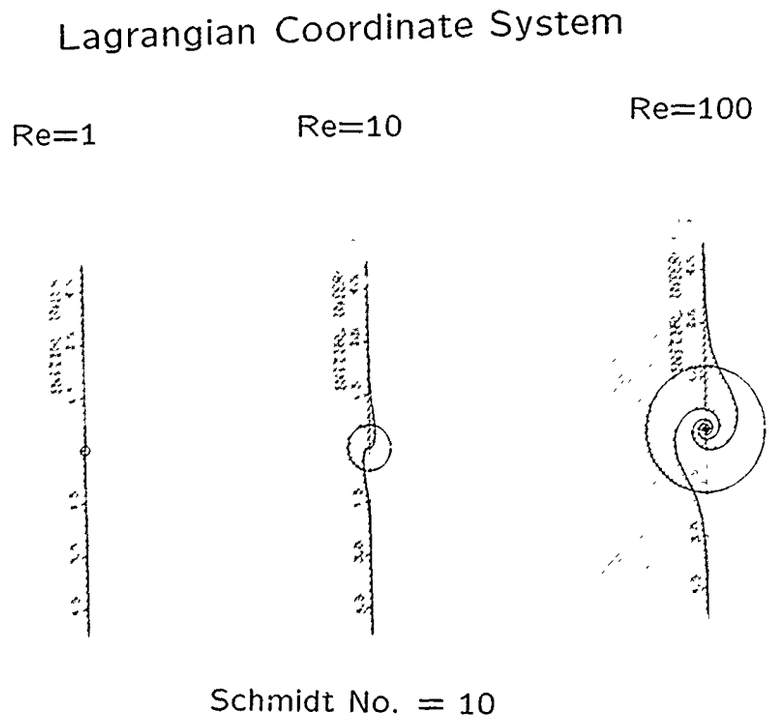

FIGURE 3 Plots of the interface shape for three values of the Reynolds number, 1, 10 and 100, in a Lagrangian coordinate system as determined by the large Schmidt number asymptotic analysis: these plots were calculated for a Schmidt number of 10, which satisfies the requirements of this analysis. The circle around the origin shows the radius at which the burnt core is located as discussed in the text.

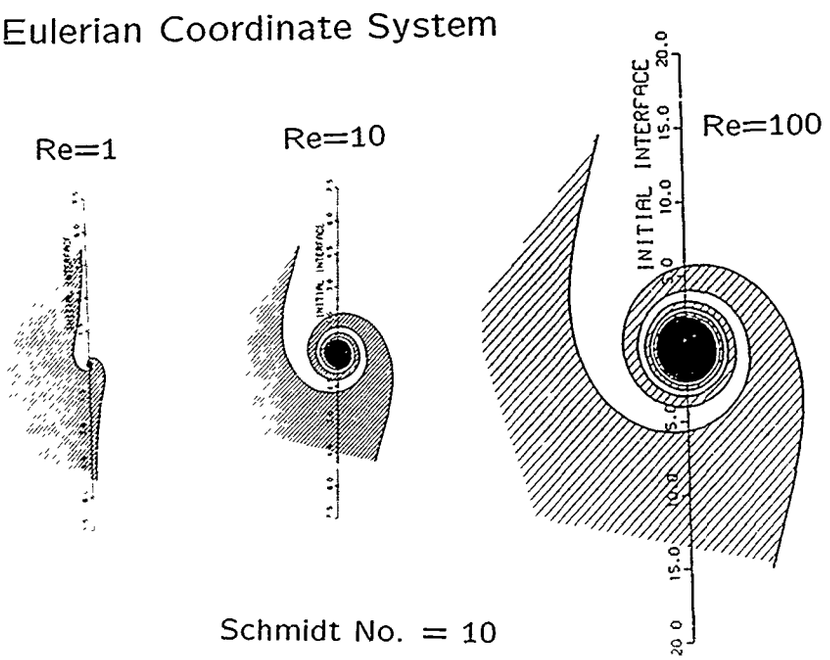

FIGURE 4 Plots of the interface shape in Eulerian coordinates for the same conditions shown in Figure 3. In each plot, the area within the burnt core has been blackened. The amount of convective mixing and the distance from the origin at which the interface deviates from planar increases dramatically with Reynolds number.

of the interface is in the direction opposite to that of the convective mixing, which is positive in the counterclockwise direction. This is because the mixing increases the gradients between fuel and oxidizer, enhancing counterrotation diffusion. Note furthermore that the deviations of the interface from planar outside of the burnt core is very small, showing that beyond the burnt core the interface between fuel and oxidizer is essentially controlled by the convective mixing.

In Figure 4 is shown plots of the interface shape in Eulerian coordinates for the same three values of Reynolds number and for the Schmidt number shown in Figure 3. These plots are drawn approximately to scale, so that structures formed at larger Reynolds number extend to larger radius (or similarity variable η). In each plot the area has been blackened within the burnt core to indicate no reaction activity. As in Figure 3, the burnt core grows with increasing Reynolds number. The amount of convective mixing in the counterclockwise direction increases dramatically with Reynolds number; both the radial distance from the origin at which the interface deviates from planar and the winding of the interface inside of this radial location are substantially larger for $Re = 100$ than for $Re = 10$.

Two points should be noticed for all plots of the solutions, both asymptotic and numerical, of the Marble problem. First, these plots do not represent the time evolution or convective mixing of a particular instance of the problem, even though the sequence gives this illusion. Second, the time evolution of any one example of the problem, *i.e.*, one Reynolds number, can be visualized as follows. The interface shape is a curve or functional relation between θ and η, and any location on this interface is given by a specific pair η, θ. Since $\eta = r^2/4\nu t$, a particular location on the interface at one time t will determine a radial position r. At a later time, the interface shape does

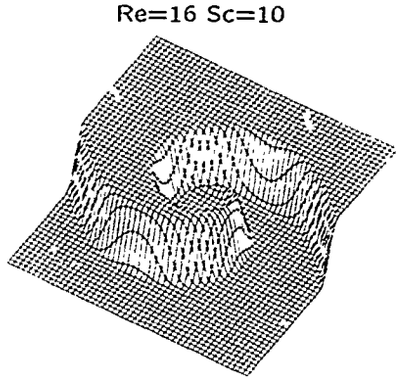

FIGURE 5 Perspective plot of the mixture-fraction surface for $Re = 16$ and $Sc = 10$. The mixture fraction ranges between zero (oxidizer) and one (fuel), with one half being the value when combustion is complete

not change and this location will "diffuse" out to a new radial position determined by the condition that η remains constant. Therefore, the interface will retain the same shape, determined by the η, θ relation as time increases, but the length scale characterizing the interface will increase as $r \propto \sqrt{t}$.

Other graphical displays of the asymptotic solution have been utilized to visualize the nature of the solution for the mixture fraction. One of these is a perspective plot of the mixture fraction as a function of the spatial coordinates. Another is color raster or pixel plots of the mixture fraction as a function of the spatial coordinates. Here, the color is used to denote the size of the mixture-fraction variable. Each of these plots is shown in an Eulerian reference frame.

In Figure 5, a perspective plot of the mixture fraction is presented for the Reynolds number equal to sixteen and the Schmidt number equal to ten. The mixture fraction ranges between zero (oxidizer) and one (fuel), with one half being its value when combustion is complete for an initially stoichiometric ratio of fuel and oxidizer. Figure 5 shows the fuel and oxidizer being mixed by convection, with a sharp diffusion-controlled transition between the two. In the center of the figure is a small circular region where the value of the mixture fraction is one half; in this region the combination of convective mixing and diffusion have caused complete combustion in the stoichiometric case. This plot was prepared using a 49 × 49 grid, which is adequate resolution for these values of the Reynolds and Schmidt numbers.

In Figure 6, a perspective plot of the mixture fraction is presented for a Reynolds number of 50 and a Schmidt number of 10. The larger Reynolds number has clearly caused much more extensive convecting winding, and the 49 × 49 grid used for the plot is now barely adequate for resolving the surface, particularly near the center where the winding is most intense. This observation brings up an important point concerning resolution. The plots in Figures 5 and 6 have been prepared using Eqs. (17) and (18) for the mixture fraction. Since these expressions are smooth functions of the spatial coordinates, the resolution of the mixture-fraction surface is strictly determined by the grid used for plotting. If the surface had been determined by numerical computations, *e.g.*, finite-difference or spectral computations, then the grid used to compute the solution would have been the determing resolution factor.

Figures 7 and 8 illustrate this point. Both figures are the mixture-fraction surface with parameters $Re = 100$ and $Sc = 10$, but Figure 7 is for a 49 × 49 plotting grid while Figure 8 is for 99 × 99 grid. Note that both figures capture the nature of

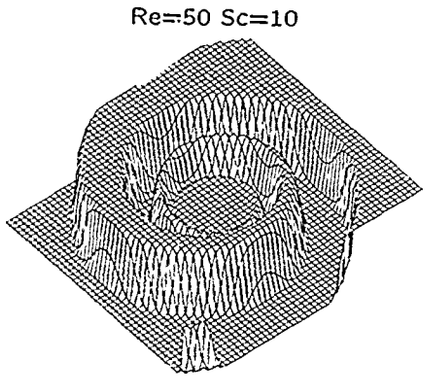

FIGURE 6 Perspective plot of the mixture-fraction surface for $Re = 50$ and $Sc = 10$. The mixture fraction ranges between zero (oxidizer) and one (fuel), with one half being the value when combustion is complete.

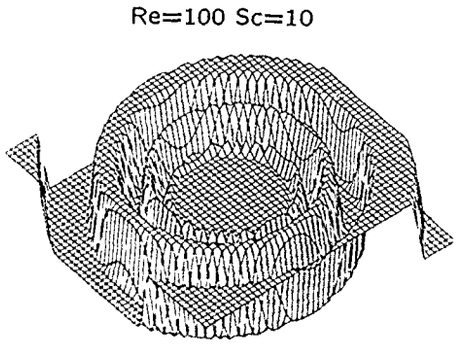

FIGURE 7 Perspective plot of the mixture-fraction surface for $Re = 100$ and $Sc = 10$. This plot was prepared using a grid of 49×49.

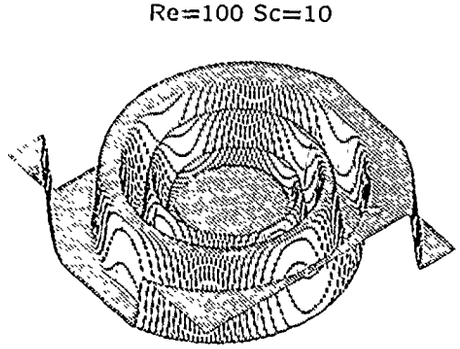

FIGURE 8 Perspective plot of the mixture-fraction surface for $Re = 100$ and $Sc = 10$. This plot was prepared using a grid of 99×99.

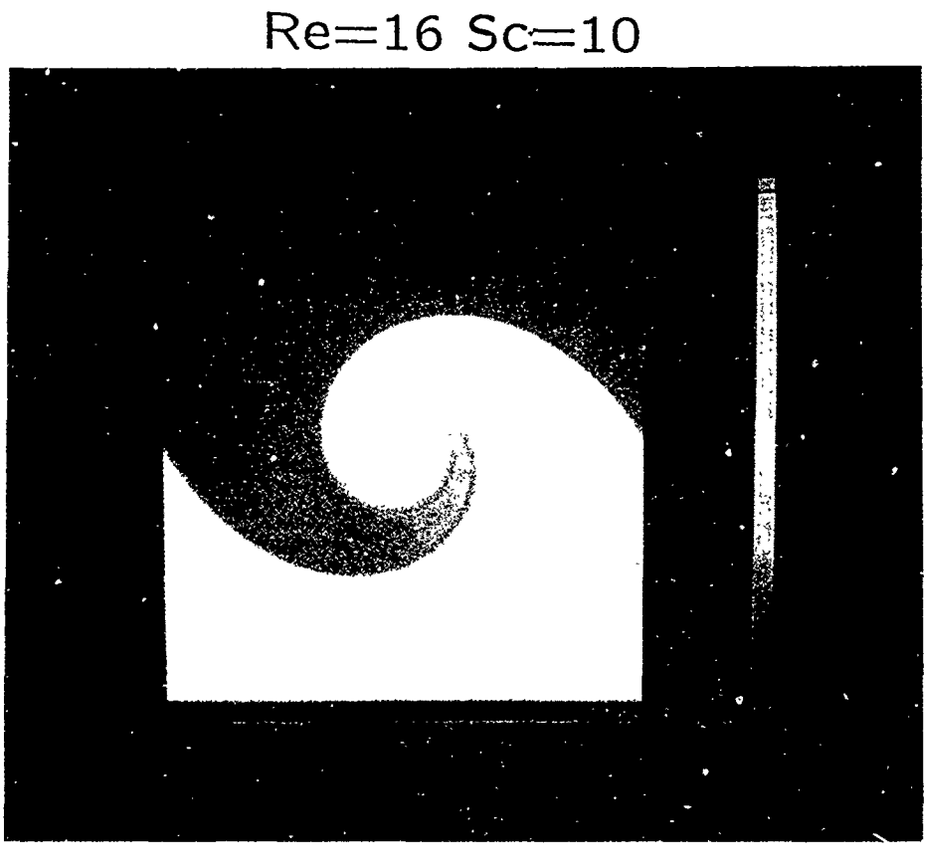

FIGURE 9 The mixture fraction displayed using a color raster plot with 1000 × 1000 resolution. Here a color is assigned to the size of the mixture fraction, blue is assigned to fuel and white to oxidizer. A band of yellow, centered at the value of 1/2 and blended into the other two colors, has been imposed on the figure to highlight the region where the gradients are large and combustion takes place. For this case $Re = 16$ and $Sc = 10$.

the mixture-fraction surface with its increased convective mixing and larger central circular region of complete combustion compared to cases with smaller Reynolds numbers. However, although the coarser grid captures the behavior of the surface, it depicts a surface which is rough in spots, particularly near the center, where the highest resolution is required to follow the winding. In Figure 8, on the other hand, there is enough resolution to capture smoothly the behavior of the mixture-fraction surface.

An alternate, and we believe preferable, method for displaying such results is to assign a color to the height of the mixture-fraction surface as shown in Figures 9 and 10. In Figure 9, $Re = 16$ and $Sc = 10$ and in Figure 10, $Re = 200$ and $Sc = 10$. The resolution of each figure is 1000 × 1000. Blue designates fuel and white oxidizer. A band of yellow, centered at the value 1/2 of the mixture fraction and blended into the blue and the white, has been imposed on the figures to highlight the region where the gradients of the mixture fraction are largest and where the combustion takes place. The resolution is oustanding as can be seen in Figure 10 where the convective winding is intense.

3.2 *Numerical Solution*

Numerical solution of Eq. (7) has been performed for many values of the parameters Re and Sc using a central difference approximation to the differential operators.

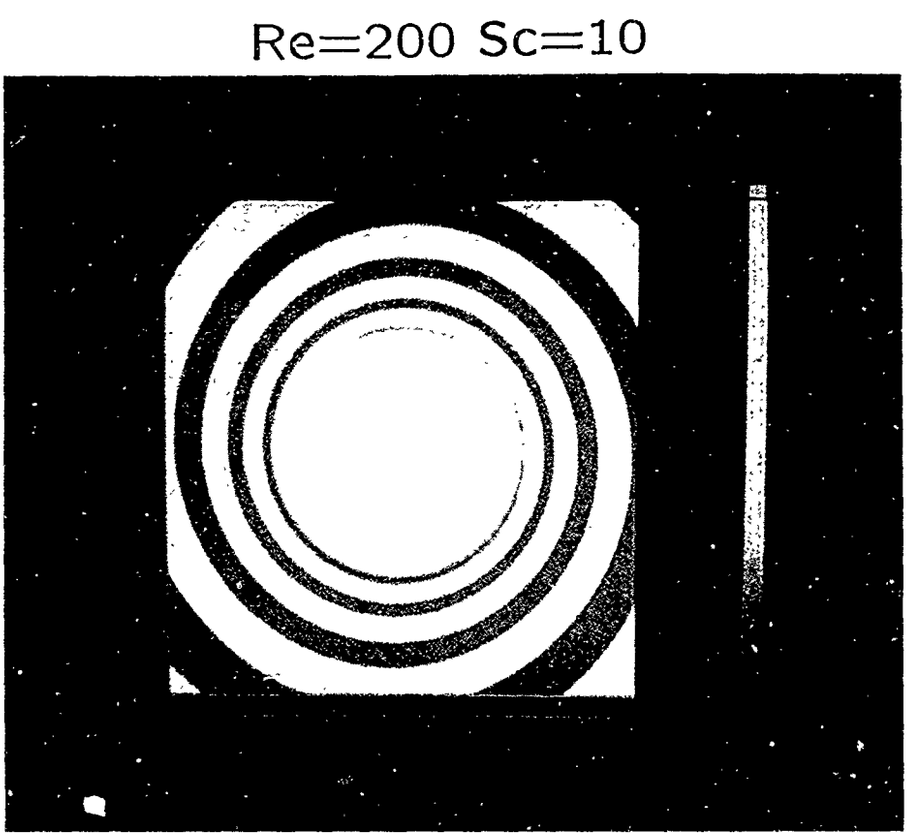

FIGURE 10 The mixture fraction displayed using a color raster plot with 1000 × 1000 resolution. Here a color is assigned to the size of the mixture fraction; blue is assigned to fuel and white to oxidizer. A band of yellow, centered at the value of 1/2 and blended into the other two colors, has been imposed on the figure to highlight the region where the gradients are large and combustion takes place. For this case $Re = 200$ and $Sc = 10$

The interval of integration for the differential equation is truncated to carry out the numerical integration and asymptotic values for the Fourier amplitudes are applied at the truncated location. A finite number of Fourier modes has been computed, and, as noted above, only odd modes of integer greater than zero have been computed. The analytical behavior of the solution for small values of the independent variable η must be handled carefully for lower order modes; therefore, a different dependent variable is computed near the origin. The pure diffusion case, when $Re = 0$, has been used to assess accuracy, particularly the effects of the finite truncation value, the number of Fourier modes and the number of grid points in the finite difference scheme required for a specified resolution. All computations reported here are for $0 \leqslant \eta \leqslant 10$ and for 19 Fourier sine and cosine modes. The inner location at which a different dependent variable is computed is $\eta = 1$.

3.3 *Comparison of Asymptotic and Numerical Results*

The numerical computations have been performed for many value of the Reynolds number and the Schmidt number. For values of these parameters of order one, the numerical calculations are straightforward, accurate and converge well. However, for

larger values of these parameters, the computations require more care to ascertain the quality of the results. For larger Schmidt numbers, this is because the interface between fuel and oxidizer becomes sharper due to the reduction in the diffusion coefficient D. As the Reynolds number is increased, the convective mixing causes the mixture-fraction to become more tightly wound within a specified value of η (radius) and also causes the maximum value of η over which mixing occurs to become larger, requiring the calculations to be carried out to larger values of η for a particular accuracy. Therefore, the large Schmidt number analysis is very useful for both examining the structure of the solution and obtaining accurate solutions for large Reynolds numbers.

We performed a series of computations to assess the quality of the asymptotic and numerical solutions as functions of the Reynolds and Schmidt numbers. The numerical solution was determined and compared with the values of the asymptotic solution at the same locations. A convenient way to do this is to fix a value of η and to compare the numerical and asymptotic solutions as a function of angle θ. To make these comparisons more accurately, we calculated and plotted the mixture fraction minus one half, and these plots are shown below. Such comparisons provide both qualitative and quantitative information on the relationship between the two solutions. We note that the two solutions should be regarded as complementary since the numerical solution will be easier to obtain and more accurate at small values of the parameters, whereas the asymptotic solutions will be valid and more accurate for larger values of the Reynolds and Schmidt numbers.

In Figure 11a–d are shown comparisons between the numerical and the asymptotic solutions as functions of angle for four values of η, 0.5, 1.0, 5.0 and 9.0, when $Re = 1$ and $Sc = 10$. The numerical solution is the solid line in each case, and the asymptotic solution is the dotted line. For all values of η and θ the two solutions are seen to agree within about ten percent.

In Figures 12a–d comparisons between the two solutions are shown at the same values of η as in the previous case, but now for $Re = 1$ and $Sc = 1$. We note that the quantitative comparisons are not as good, particularly at the smallest value of η, but that qualitatively, both solutions agree. For values of η greater than 1/2, the two solutions are seen to agree to within about twenty percent, a remarkable fact considering that the asymptotic analysis requires that the Schmidt number be large compared to unity.

Similar comparisons have been made for several other values of the Reynolds number for Schmidt numbers of one and ten. Examination of these results shows that the agreement between the numerical and asymptotic solutions are quite good. For $Re = 16$ and $Sc = 10$, for example, the comparison plots at $\eta = 5.0$ and $\eta = 9.0$ differ only slightly quantitatively from those shown in Figure 12c and d. At the smaller values of η for this Reynolds and Schmidt numbers, the agreement is poorer, but, at these values, the mixture fraction is relatively small, ranging between ± 0.2. In Figures 13a and b, comparisons are made at $\eta = 5.0$ and $\eta = 9.0$ for $Re = 16$ and $Sc = 1$. Although there is good quantitative agreement at $\eta = 9.0$, the solutions agree only qualitatively at $\eta = 5.0$. However, for $\eta = 0.5, 1.0$ for these values of the Reynolds and Schmidt numbers, the numerical and the asymptotic solutions indicate that the mixture fraction minus one half is zero to within ± 0.015.

Finally, comparisons have been made at several values of η for $Re = 100$ and for $Sc = 10$ and $Sc = 1$. For these values of the Reynolds and Schmidt numbers, the mixture fraction is found by both solution techniques to be 1/2 for $\eta = 0.5$ and $\eta = 1.0$. At $\eta = 5.0$ the agreement between the asymptotic and the numerical solutions, using the resolution described earlier for the numerical computations, is found to be poor for both values of the Schmidt number. In Figures 14a and b are shown the mixture fraction minus one half at $\eta = 9.0$ for $Re = 100$ for

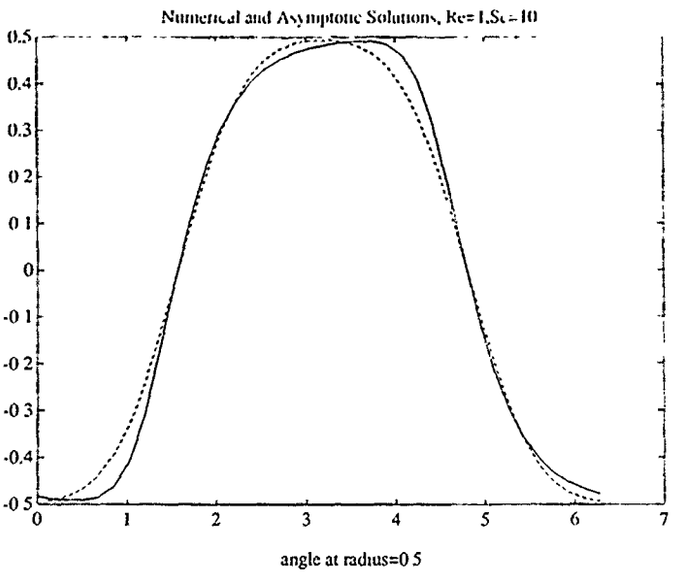

(a)

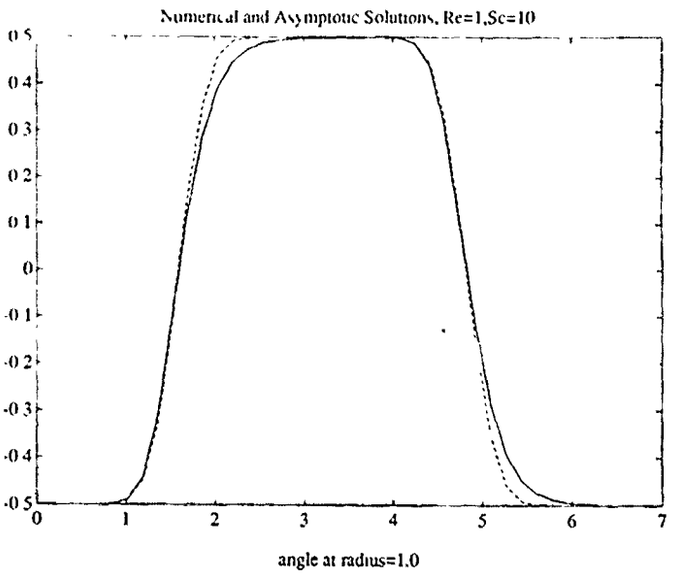

(b)

FIGURE 11 Comparisons between the numerical (solid line) and asymptotic (dashed line) solutions with parameters $Re = 1$ and $Sc = 10$ at four values of the similarity variable η. (a) $\eta = 0.5$, (b) $\eta = 1.0$, (c) $\eta = 5.0$ and (d) $\eta = 9.0$.

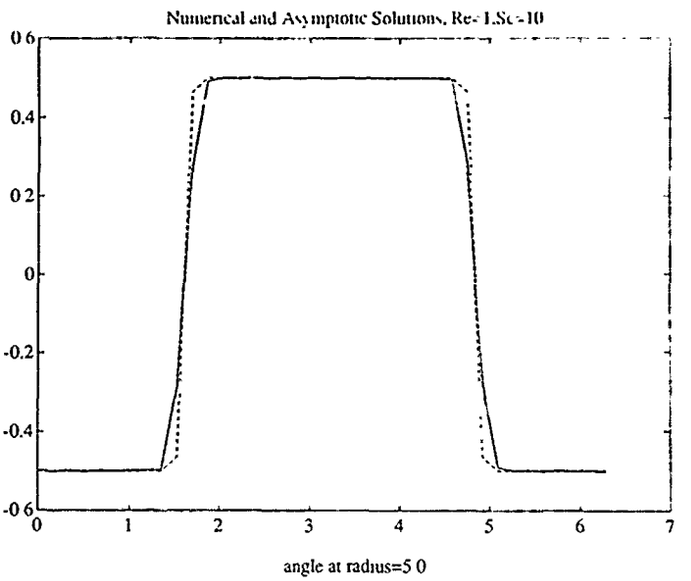

(c)

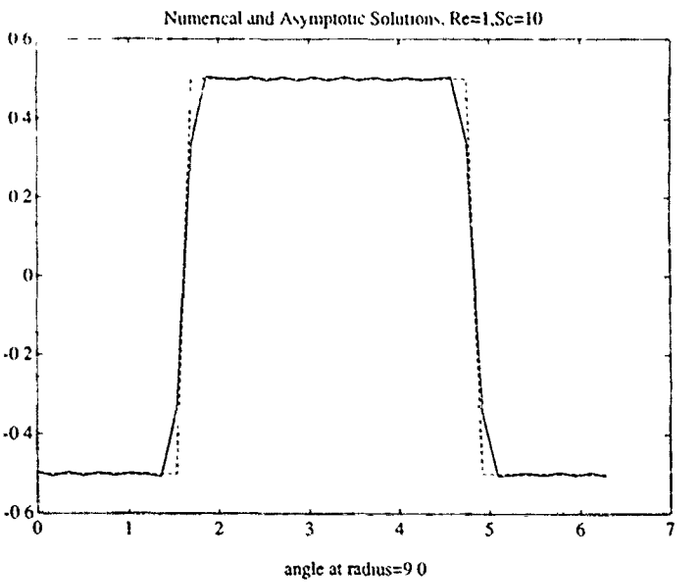

(d)

FIGURE 11 continued.

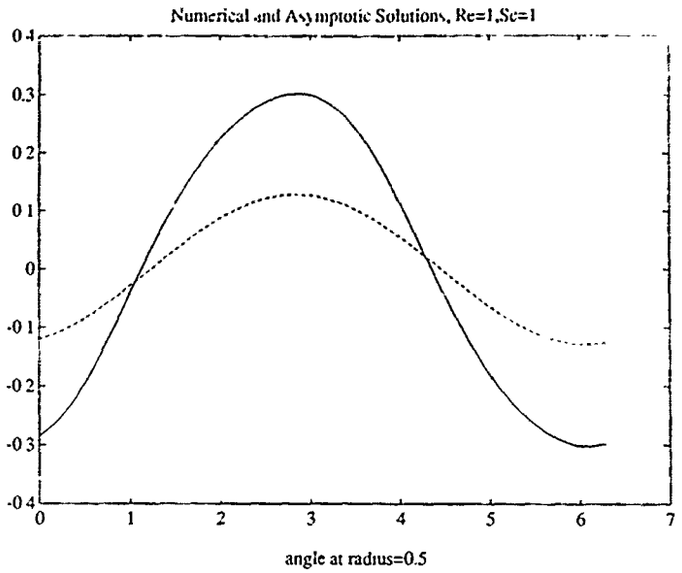

(a)

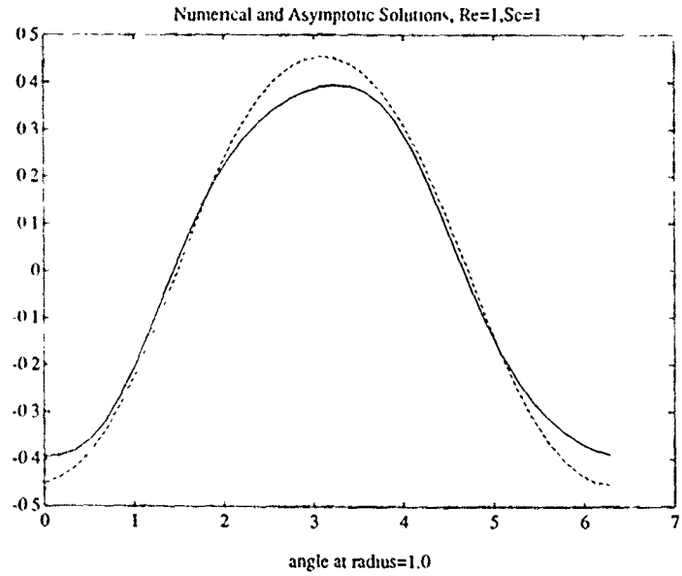

(b)

FIGURE 12 Comparisons between the numerical (solid line) and asymptotic (dashed line) solutions with parameters $Re = 1$ and $Sc = 1$ at four values of the similarity variable η (a) $\eta = 0.5$, (b) $\eta = 1.0$, (c) $\eta = 5.0$ and (d) $\eta = 9.0$

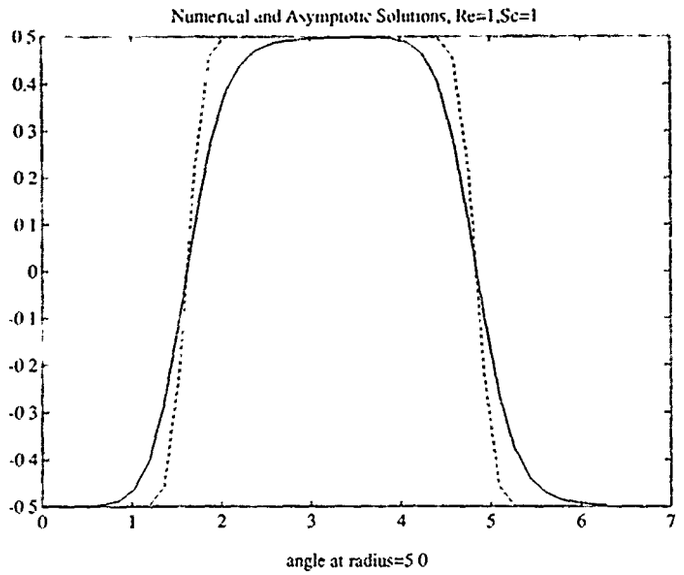

(c)

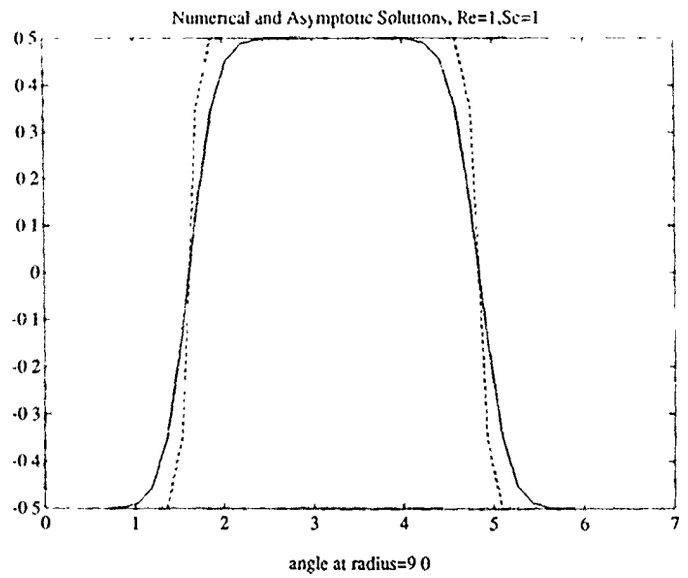

(d)

FIGURE 12 continued.

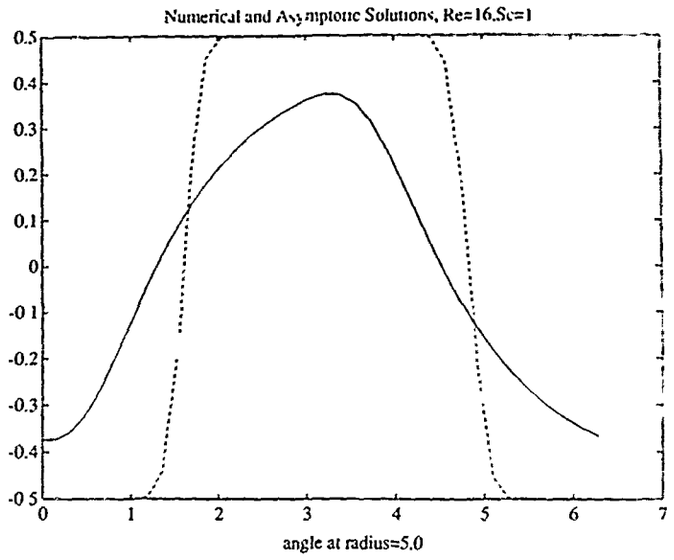

(a)

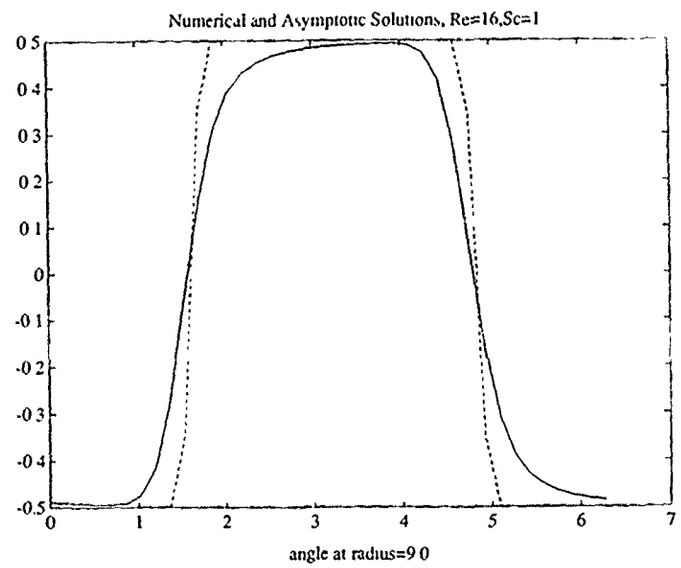

(b)

FIGURE 13 Comparisons between the numerical (solid line) and asymptotic (dashed line) solutions with parameters $Re = 16$ and $Sc = 1$ at two values of the similarity variable η (a) $\eta = 5.0$ and (b) $\eta = 9.0$.

$Sc = 10$ and $Sc = 1$ respectively. In both cases, quantitative agreement is reasonably good. For these values of the governing parameters (Re and Sc), the asymptotic solution is probably more reliable for the resolution used for the numerical solutions.

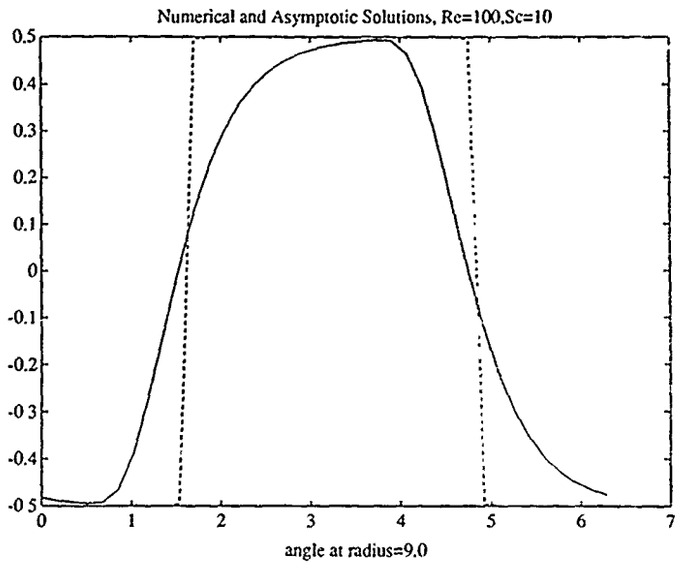

(b)

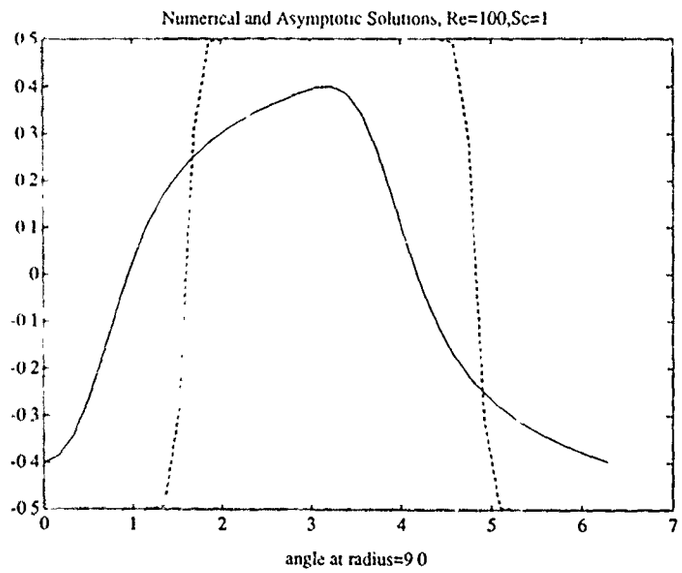

(a)

FIGURE 14 Comparisons between the numerical (solid line) and asymptotic (dashed line) solutions at a single value of the similarity variable $\eta = 9.0$ (a) $Re = 100$, $Sc = 10$, and (b) $Re = 100$, $Sc = 1$

4 CONSUMPTION RATE

Important quantities of interest from this analysis are the global consumption rates for fuel and oxidizer and the global rate of heat release; it is desired to calculate these quantities as functions of the Reynolds number, Schmidt number and initial

concentrations of fuel and oxidizer. The consumption rates under general conditions can be calculated from the analysis presented earlier but require computation of Fourier amplitudes using an ODE solver, synthesis of the solution using FFT routines, location of the flame surface using a root finder and integration over the whole sheet to obtain the global rates.

The local rates of consumption of fuel and of oxidizer and the rate of heat release are all proportional to the derivative of Z normal to the flame surface. Therefore, the calculation of these quantities requires us first to locate the flame sheet and then to determine the derivative of the Z normal to it. Numerically, this can be inaccurate. When the Schmidt number is large, the analytical results of Subsection 3.1 can be used both to locate the flame sheet and to obtain an expression for the normal derivative of Z. When the initial mixture of fuel and oxidizer is stoichiometric, the flame sheet occurs at $Z = 1/2$ and is located along the curves determined in Lagrangian coordinates by $\Phi_0 = 0$ (Eqs. (18)). These lines are transformed by Eqs. (6) into the Eulerian system:

$$0 = \pm \frac{\pi}{2} + \frac{Re}{2Sc} \tilde{f}_2(\eta) + \frac{Re}{2\eta} [1 - E_2(\eta)] \tag{19}$$

The flame sheet then consists of two curves each of the form $\theta(\eta)$.

The gradient of Z in cylindrical coordinates can be found in Lagrangian coordinates using Eq. (6) and then in terms of the similarity variables $\eta = r^2/(4\nu t)$, θ_0 (where we note that the Lagrangian variables ϱ and τ can be replaced by r and t). The analytical expression Eq. (17) for $\tilde{Z}$ can be differentiated and evaluated along the flame sheet $\Phi_0 = 0$. The consumption rates of fuel and oxidizer locally are

$$dC = D \frac{dZ}{dn} ds = D\boldsymbol{n} \cdot \boldsymbol{Z} ds \tag{20}$$

where D is the species diffusion coefficient, n is the normal direction to the flame sheet, and s is the arc length along the flame sheet. Then the total consumption rate for either species is

$$C = D \int_{\text{flame sheet}} \frac{dZ}{dn} ds \tag{21}$$

One additional complication arises at this point. Either with or without a vortex, the consumption rate is infinite because there is an infinite length over which the reaction takes place Therefore, we determine the enhancement caused by the imposition of the vortex. If we denote by C_0 the consumption rate in the pure diffusion case ($Re = 0$), then we desire $C - C_0$.

Calculation of the consumption rate enhancement generally would require numerical integration. In an attempt to push the analytical calculations as far as possible and to obtain expressions with which to compare those derived by Marble and Karagozian (1982, 1985, 1986) we further assume that the Reynolds number is large. A large Reynolds number is one for which the functions $\tilde{A}_m(\eta; Re, Sc)$ appearing in the exponential amplitudes in the asymptotic solution Eq. (17) are large enough that these amplitudes are small; then the terms in the Fourier series decrease very rapidly with increasing m and for our purposes, the Fourier series can be approximated by only one term. Therefore, for $m = 1$, we require that $\tilde{A}_1 \geqslant 3$ approximately; a

Reynolds number of 100 or more is adequate for example. Then, the asymptotic expressions for $\tilde{f}_1$ and $\tilde{f}_2$ for large η, which were given earlier, can be used. Using only the first term in the Fourier series solution Eq. (17) and taking only the "large η" expression for the equation for the flame sheet and for the Eulerian–Lagrangian transformation, we find relatively simple expressions for the normal derivative of the mixture fraction and for the arc length along the flame sheet for a stoichiometric mixture. Integration of the approximate expression for the local enhancement of the consumption rate over the flame sheet then gives the global enhanced species consumption rate:

$$C - C_0 \approx \frac{\tilde{\Gamma}(2/3)}{\pi} D \left(\frac{2Re^2Sc^2}{3} \right)^{1/3} \tag{22}$$

Details of this calculation can be found in Rehm (1987). We note that the parametric dependence of this expression agrees with that reported by Marble and Karagozian (1982, 1985, 1986).

5 CONCLUSIONS

The reaction of two species occupying adjacent half spaces initially and mixed convectively by an imposed vortex is a fundamental problem. It provides a situation in which the competing processes of convection, diffusion and reaction can be examined in a simple setting. In this paper we analyzed the problem by analytical methods that accurately solve the equations globally. An important result is the large-Schmidt-number asymptotic solution for the mixture fraction. Other results are a methodology for solving this problem by numerical methods, plots of the solution as a function of the governing parameters, Reynolds and Schmidt numbers, and the dependence of the consumption rate on these parameters for large values. The plots confirm the behavior of the solution found numerically by Laverdant and Candel (1988), and the consumption-rate dependence corroborates that found by Marble (1985).

The key features of the analysis are the observations that the problem permits a global similarity solution and that the equations can be transformed to Lagrangian coordinates. The first observation reduces the number of independent variables from three to two, and the second eliminates scaling difficulties arising in convection-diffusion equations when the Reynolds number is large. The Marble problem is inherently interesting because it addresses the question of enhancement of species consumption and heat release rates by flame stretching in a simple geometry. It is also of interest because it simulates the enhancement in these rates in a vortex generated in a two dimensional shear layer.

Comparisons between the asymptotic solution and numerical solution of the Marble problem indicate that the asymptotic solution is remarkably good. We have noted that these two solutions are complementary; where one solution is better the other is poorer, but exactly where this trade-off occurs has not been determined. In particular, the numerical solution is best for small values of the Schmidt and Reynolds numbers, while the asymptotic solution is best for large values of these parameters.

This problem can clearly be extended in several directions. Obvious directions for generalization are to consider other flow fields, more general geometries for the initial fuel and oxidizer configurations, and the effects of density changes induced by heat release on mixing. Using the same type of local analysis originally employed by Marble, a more general flow field and density variations have been considered

analytically by Karagozian and Marble (1982, 1986) and the effects of finite-rate chemistry have been examined by Norton (1983). A more general flow and generalized species geometries were investigated analytically in the paper by Baum, Corley and Rehm (1986). These generalizations were also the subject of investigation by numerical techniques by Riley, Metcalfe and Orszag (1986), McMurtry et al. (1986), McMurtry and Riley (1987), Ghoniem and Givi (1987) and Laverdant and Candel (1988).

Dr A. Linãn has indicated in a private communication that he has also used analytical methods to exploit the fact that the Marble problem admits a similarity solution.

ACKNOWLEDGEMENT

We wish to thank Dr G. B. McFadden for a useful discussion and comments on the paper and Dr C. Fenimore for his helpful comments. This research was partially supported by the Air Force Office of Scientific Research under Contract AFOSR-ISSA-88-0026.

REFERENCES

Ashurst, W. T. (1987). "Vortex Simulation of Unsteady Wrinkled Laminar Flames", *Combust. Sci. Technology* 52, 325.

Buckmaster, J. D. and Ludford, G. S. S. (1982). *Theory of Laminar Flames*, Cambridge University Press.

Buckmaster, J. D. and Ludford, G. S. S. (1983). *Lectures on Mathematical Combustion*, Society for Industrial and Applied Mathematics, Philadelphia, Pennsylvania.

Baum, H. R., Corley, D. M. and Rehm, R. G. (1986). "Time-Dependent Simulation of Small-Scale Turbulent Mixing and Reaction", *Twenty-First Symposium (International) on Combustion*, The Combustion Institute, pp. 1263-1270.

Brown, G. L. and Roshko, A. (1974). "On Density Effects and Large Structure in Turbulent Mixing Layers", *J. Fluid Mech* 91, 319.

Browand, F. K. (1986). "The Structure of the Turbulent Mixing Layer", *Physica* 18D, 135.

Carrier, G. F., Fendell, F. E. and Marble, F. E. (1975). "The Effect of Strain Rate on Diffusion Flames", *SIAM J. Appl. Math.* 28, No. 2, March.

Ghoniem, A. F. and Givi, P. (1987). "Vortex-Scalar Element Calculations of a Diffusion Flame", Paper AIAA-87-0225, paper presented at the *AIAA 25th Aerospace Sciences Meeting*, Reno, Nevada.

Karagozian, A. R. and Marble, F. E. (1986) "Study of a Diffusion Flame in a Stretched Vortex", *Comb. Sci. Tech.* 45.

Karagozian, A. R. (1982). "An Analytical Study of Diffusion Flames in Vortex Structures", Ph.D. Thesis, California Institute of Technology, Pasadena, Cal.

Laverdant, A. M. and Candel, S. M. (1988a) "A Numerical Analysis of a Diffusion Flame-Vortex Interaction", *Comb. Sci. Tech.* 60, 79.

Laverdant, A. M. and Candel, S. M. (1988b). "Etude de L'Interaction de Flammes de Diffusion et de Premelange avec un Tourbillon", *La Recherche Aerospatiale* 3, 13.

Libby, P. A. and Williams, F. A. (eds.), (1980). *Turbulent Reacting Flows*, Springer-Verlag, Berlin.

Marble, F. E. (1985). "Growth of a Diffusion Flame in the Field of a Vortex", *Recent Advances in Aerospace Sciences* (C. Casci, Ed.) 315.

McMurtry, P. A., Jou, W.-H., Riley, J. J. and Metcalfe, R. W. (1986). "Direct Numerical Simulations of a Reacting Mixing Layer with Chemical Heat Release", *A.I.A.A. Journal* 24, 962.

McMurtry, P. A. and Riley, J. J. (1987) "Mechanisms by Which Heat Release Affects the Flow Field in a Chemically Reacting, Turbulent Mixing Layer", Paper AIAA-87-0131, paper presented at the *AIAA 25th Aerospace Sciences Meeting*, January 12-15, Reno, Nevada.

McMurtry, P. A. (1987). "Direct Numerical Simulations of a Reacting Mixing Layer with Chemical Heat Release", Ph.D. Thesis, Mechanical Engineering, University of Washington, Seattle, Washington.

Mungal, M. G. and Dimotakis, P. E. (1984). "Mixing and Combustion with Low Heat Release in a Turbulent Shear Layer", *J. Fluid Mech.* 148, 349.

Norton, O. P. (1983). "The Effects of a Vortex Field on Flames with Finite Reaction Rates", Ph.D. Thesis, California Institute of Technology, Pasadena, Cal.

Oppenheim, A. K. (1986). "The Beauty of Combustion Fields and Their Aerothermodynamic Significance", *Dynamics of Reactive Systems Part I. Flames and Configurations*, J. R. Bowen, J.-C. Leyer and R. I. Soloukhin (eds), Progress in Astronautics and Aeronautics, Vol. 105, A.I.A.A., 1633 Broadway, N.Y., N.Y. 10019.

Oran, E. S. and Boris, J. P. (1981). Detailed Modelling of Combustion Systems, *Prog. Energy Combust. Sci.* 7, 1.

Peters, N. (1984). "Laminar Diffusion Flamelet Models in Non-Premixed Turbulent Combustion", *Prog. Energy Combust. Sci.* 10, 319.

Rehm, R. G., Baum, H. R. and Lozier, D. W. (1986). "Two-Dimensional Flame in a Vortex Field", Paper presented at the *SIAM 1986 National Meeting*, Boston, Mass.

Rehm, R. G., Baum, H. R. and Lozier, D. W. (1987). "Diffusion-Controlled Reaction in a Vortex Field", National Bureau of Standards Report NBSIR 87-3572.

Riley, J. J., Metcalfe, R. W. and Orszag, S. A. (1986). "Direct Numerical Simulations of Chemically Reacting Mixing Layers", *Phys. Fluids* 29, 406.

Roshko, A. (1976). "Structures of Turbulent Shear Flows: A New Look", *A.I.A.A. Journal* 14, 1349.

Williams, F. A. (1985). *Combustion Theory, The Fundamental Theory of Chemically Reacting Flow Systems*, Second Edition, The Benjamin/Cummings Publishing Co., Inc., Menlo Park, California.